University of Hertfordshire UH 25 Research Archive

Citation for published version:
Chiaki Kobayashi, Miho N. Ishigaki, Nozomu Tominaga, and Ken'ichi Nomoto, 'THE ORIGIN OF LOW [α/Fe] RATIOS IN EXTREMELY METAL-POOR STARS', *The Astrophysical Journal Letters*, Vol. 785(L5), April 2014.

DOI:
http://dx.doi.org/10.1088/2041-8205/785/1/L5

Document Version:
This is the Published Version.

Copyright and Reuse:
© 2014 American Astronomical Society.

Content in the UH Research Archive is made available for personal research, educational, and non-commercial purposes only. Unless otherwise stated, all content is protected by copyright, and in the absence of an open license, permissions for further re-use should be sought from the publisher, the author, or other copyright holder.

Enquiries
If you believe this document infringes copyright, please contact the Research & Scholarly Communications Team at rsc@herts.ac.uk

The Astrophysical Journal Letters, 785:L5 (5pp), 2014 April 10 doi:10.1088/2041-8205/785/1/L5
© 2014. The American Astronomical Society. All rights reserved. Printed in the U.S.A.

THE ORIGIN OF LOW [α/Fe] RATIOS IN EXTREMELY METAL-POOR STARS

Chiaki Kobayashi[1,2], Miho N. Ishigaki[2], Nozomu Tominaga[2,3], and Ken'ichi Nomoto[2]
[1] School of Physics, Astronomy and Mathematics, Centre for Astrophysics Research, University of Hertfordshire, College Lane, Hatfield AL10 9AB, UK; c.kobayashi@herts.ac.uk
[2] Kavli Institute for the Physics and Mathematics of the Universe (WPI), The University of Tokyo, Kashiwa, Chiba 277-8583, Japan
[3] Department of Physics, Faculty of Science and Engineering, Konan University, 8-9-1 Okamoto, Kobe, Hyogo 658-8501, Japan
Received 2013 November 19; accepted 2014 March 7; published 2014 March 25

ABSTRACT

We show that the low ratios of α elements (Mg, Si, and Ca) to Fe recently found for a small fraction of extremely metal-poor stars can be naturally explained with the nucleosynthesis yields of core-collapse supernovae, i.e., 13–25 $M_\odot$ supernovae, or hypernovae. For the case without carbon enhancement, the ejected iron mass is normal, consistent with observed light curves and spectra of nearby supernovae. On the other hand, the carbon enhancement requires much smaller iron production, and the low [α/Fe] of carbon-enhanced metal-poor stars can also be reproduced with 13–25 $M_\odot$ faint supernovae or faint hypernovae. Iron-peak element abundances, in particular Zn abundances, are important to put further constraints on the enrichment sources from galactic archaeology surveys.

Key words: galaxies: abundances – galaxies: evolution – stars: abundances – stars: Population III – supernovae: general

Online-only material: color figures

1. INTRODUCTION

The observed elemental abundances of metal-poor stars can be used to constrain the physics of supernovae (see Nomoto et al. 2013 for a review). Although the nature of the first stars is not well understood, if they explode as supernovae, the first chemical enrichment is imprinted in the elemental abundances of the second generation of stars. During the early stages of galaxy formation, the interstellar medium (ISM) is highly inhomogeneous, and it is likely that these elemental abundance patterns are determined only by a few supernovae (Audouze & Silk 1995). In inhomogeneous enrichment, metallicity is no longer a time indicator but merely reflects the metallicity of the cloud where the second generation of stars formed. This metallicity is often estimated with an analytic formula (Tominaga et al. 2007b), but detailed hydrodynamical simulations with radiative cooling are necessary to predict the metallicity distribution function of the second generation of stars. Alternatively, we assume that metal-poor stars with [Fe/H] $\lesssim -3$ are enriched by a single supernova, and study the properties of the supernova by comparing the observed elemental abundances and nucleosynthesis yields (abundance profiling/fitting).

Thanks to large-scale surveys and follow-up high resolution spectroscopy, intensive observations of metal-poor stars have revealed the existence of extremely-, ultra-, and hyper-metal-poor (EMP, UMP, and HMP) stars with [Fe/H] = $(-4, -3)$, $(-5, -4)$, $(-6, -5)$, respectively (Beers & Christlieb 2005). The elemental abundance patterns have a distinct signature: including two HMP stars, 10%–25% of stars with [Fe/H] $\lesssim -2$ show carbon enhancement relative to iron ([C/Fe] $\gtrsim 1$, Aoki 2010). Such carbon-enhanced metal-poor (CEMP) stars often show enhancement of α elements (O, Mg, Si, S, and Ca), although one star at [Fe/H] = -4.99 does not show enhancement of C, N, and Mg (Caffau et al. 2011). There are various scenarios to explain the carbon enhancement, including rotating massive stars (Meynet et al. 2006), asymptotic giant branch stars in binary systems (Suda et al. 2004; Lugaro et al. 2008), and black-hole-forming core-collapse supernovae (faint supernovae; Umeda & Nomoto 2002; Iwamoto et al. 2005; Tominaga et al. 2007b). Caffau et al. (2013) recently presented different types of EMP stars with/without carbon enhancement that have [α/Fe] ratios lower than other EMP stars. The variation of the [α/Fe] ratios of EMP stars is known. As the quality of data improved, Cayrel et al. (2004) concluded that without CEMP, the scatter of elemental abundances is so small that the ISM is well mixed at the early stages of galaxy formation. However, a significant scatter is seen in other observational data (e.g., Honda et al. 2004; Yong et al. 2013; Cohen et al. 2013) and a small fraction of stars show lower [α/Fe] ratios than $\sim$0.2.

An intrinsic variation of [α/Fe] ratios can be caused by the following enrichment sources: (1) The most popular source is Type Ia supernovae (SNe Ia), which produce more Fe than α elements. Depending on the fractional contribution of core-collapse supernovae from previous populations, [α/Fe] can vary between $\sim$0.5 to ~ -0.6. However, in the case of SNe Ia, there is a time delay of the enrichment, which depends on the progenitor systems (Kobayashi & Nomoto 2009), and is $\sim$34 Myr at the shortest for 8 $M_\odot$ primary stars. Hence, it is unlikely that many EMP stars are affected by SNe Ia. (2) For less massive stars, the mantle mass that contains α elements is smaller, and thus $\sim$10–20 $M_\odot$ supernovae give lower [α/Fe] ratios than the initial mass function (IMF) weighted values of core-collapse supernova yields, i.e., the plateau values of [α/Fe]–[Fe/H] relations (Kobayashi et al. 2006, 2011). These supernovae will leave a neutron star behind, and should be very common for the standard IMF weighted for the low-mass end (e.g., Kroupa 2008). (3) Hypernovae ($E_{51} \equiv E/10^{51}$ erg $\gtrsim 10$ for $\gtrsim$25 $M_\odot$) are observationally known to produce more iron than normal supernovae ($E_{51} \sim 1$ for $\gtrsim$10 $M_\odot$) (e.g., Nomoto et al. 2003; Smartt 2009). Therefore, hypernovae can give lower [α/Fe] ratios than supernovae at a given progenitor mass. The hypernova rate is not very high at present, but can be high for low-metallicity stars because of small angular momentum loss. (4) Faint supernovae are proposed to explain the elemental abundance patterns of CEMP stars from carbon to zinc. The central parts of supernova ejecta that contain most of the iron fall back onto the black hole, while the stellar envelopes that

contain carbon are ejected as in normal supernovae. Therefore, the [C/Fe] ratio of faint supernovae is as large as that of CEMP stars. Among α elements, O and Mg are synthesized during hydrostatic burning and are located in the outskirts of ejecta. Therefore, faint supernovae often have high [(O, Mg)/Fe] ratios, depending on the mixing-fallback processes. The faint supernova scenario is also the best explanation of the observed carbon-enhanced damped Lyman α (DLA) system (Kobayashi et al. 2011). (5) Primordial stars with initial masses of $\sim$140–270 $M_\odot$ enter the electron–positron pair-instability region during the central oxygen-burning stages, where most O and Mg are transformed into Si, S, and Fe. Pair-instability supernovae produce a much larger amount of iron and higher [(Si,S)/(O,Mg)] ratios than core-collapse supernovae. Such abundance patterns have been found in neither EMP stars (e.g., Cayrel et al. 2004) nor DLA systems (Kobayashi et al. 2011).

In this Letter, we explore our supernova and hypernova models with/without mixing-fallback over a wide range of progenitor mass. We then perform abundance fitting to observed low-α stars and discuss the enrichment sources (Section 2). In Section 3 we give a more general discussion on supernovae and chemical enrichment, and we summarize our main conclusions in Section 4.

2. ABUNDANCE FITTING

We adopt progenitor star models from Umeda & Nomoto (2005) for 13, 15, 25, and 40 $M_\odot$ with the same modification of the number of electrons per nucleon, Y_e, as in Kobayashi et al. (2006). During the supernova explosion, the elements synthesized in different stellar layers should mix to some extent, and some fraction of this mixed material falls back onto the remnant. We calculate nucleosynthesis yields by using mixing-fallback models (Umeda & Nomoto 2002; Iwamoto et al. 2005; Tominaga et al. 2007b) for supernovae and hypernovae. The mass–energy relation is taken from the results of light curve fitting (Nomoto et al. 2003); $E_{51} = 1$ for 13–40 $M_\odot$ supernovae, and $E_{51} = 10$ and 30 for 25 and 40 $M_\odot$ hypernovae, respectively. We then perform the parameter search for three-dimensional spaces of the inner boundary of mixing $M_{\rm cut}$ (i.e., mass cut), the outer boundary of mixing $M_{\rm mix}$, and the ejection fraction of the mixing region f. The minimum, maximum, and steplength for each parameter are: $M_{\rm cut}$ = [iron core mass, 3 $M_\odot$, 0.1 $M_\odot$], $M_{\rm mix}$ = [$M_{\rm cut}$, MIN(CO core mass, 16 $M_\odot$), 0.1 $M_\odot$], and $\log f = [-5, 0, 0.1]$. Note that $f = 1$ corresponds to the case without mixing-fallback. We search acceptable models using the chi-squared test statistic, and the parameters of favored models that have the least χ^2 for given M and E are listed in Table 1. Acceptable models have parameters around the peaks and give similar χ^2 values.

For the three stars in Caffau et al. (2013), the observational constraints are [Mg/Fe], [Si/Fe], and [Ca I/Fe], and the detection or non-detection of [C/Fe]. Given the signal-to-noise ratio, temperature, and gravity of the two stars with no carbon detection, we estimate that [C/Fe] ratios should be lower than $\sim$1.5 from spectral synthesis, and apply this constraint. It is the iron peak elements that give a much stronger constraint on the model parameters but there are no observational estimates available for these stars. Instead, we put a constraint on the Ni abundance as [Ni/Fe] < 0.5 because [Ni/Fe] is almost zero for a wide range of metallicity (see Figure 24 of Kobayashi et al. 2006). Figure 1 shows the comparison of the elemental abundance patterns between observations and favored models.

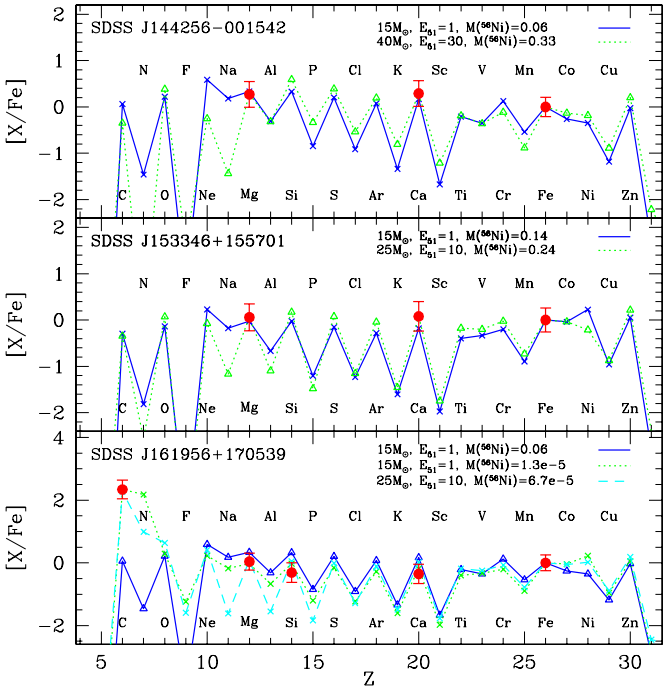

Figure 1. Elemental abundance patterns of three EMP stars with (top and middle panels) and without (bottom panel) carbon enhancement from Caffau et al. (2013). In the top and middle panels, the solid and dotted lines show the nucleosynthesis yields of a low-mass supernova without mixing-fallback and hypernova, respectively. In the bottom panel, the solid, dotted, and dashed lines are for a normal supernova without mixing-fallback, faint supernova, and faint hypernova, respectively.

(A color version of this figure is available in the online journal.)

SDSS J144256+001542—The observed [α/Fe] ratios ($\sim$0.3) are consistent with LTE abundances of typical halo stars (Cohen et al. 2013; Yong et al. 2013), but are slightly lower than the IMF-weighted yields ([Mg/Fe] $\sim$ 0.5[4] and [Ca/Fe] $\sim$ 0.3). Therefore, the observed [α/Fe] ratios can be reproduced with the yields of (1) 13–15 $M_\odot$ supernovae, (2) 13–40 $M_\odot$ supernovae with mixing-fallback, or (3) hypernovae. Among normal supernovae (with ejected iron mass M(Fe) $\sim$ 0.07 $M_\odot$), if the progenitor mass is as low as 13–15 $M_\odot$, the observed ratios can be reproduced even without mixing-fallback (solid line; see Section 1). However, 25–40 $M_\odot$ models without mixing-fallback give M(Fe) larger than observed supernovae. The remnant mass is around $M_{\rm rem} \sim 2\ M_\odot$, which is in the range of neutron stars. With mixing-fallback, the observed ratios can be reproduced with many parameter sets. However, to be consistent with observed supernovae (M(Fe) = 0.05–0.15 $M_\odot$), 40 $M_\odot$ models require extended mixing and large fallback ($M_{\rm mix} > 8\ M_\odot$ and $f < 0.3$) in order for a large fraction of the CO core to fall back, which is not very realistic (see Section 3). For hypernovae (dotted line), as we allow M(Fe) $> 0.1\ M_\odot$, [α/Fe] can be reproduced with 25–40 $M_\odot$. The remnant mass is $M_{\rm rem} \gtrsim 4\ M_\odot$, which is in the range of black holes.

SDSS J153346+155701—Although the observed [α/Fe] ratios ($\sim$0) are lower than the above stars, the ratios can be reproduced with (1) 13–15 $M_\odot$ supernovae (solid line), (2) 13–40 $M_\odot$ supernovae with mixing-fallback, or (3) hypernovae (dotted line). Compared with the above star, a smaller mass cut $M_{\rm cut}$ is favored at a given progenitor mass in order to obtain larger iron yields and thus lower [α/Fe] ratios. With mixing-fallback,

[4] This is consistent with NLTE abundances (Andrievsky et al. 2010).

Table 1

Observed Abundances, the Parameters of Nucleosynthesis Models (Progenitor Mass M, Explosion Energy E_{51}, Inner Boundary $M_{\rm cut}$, Outer Boundary $M_{\rm mix}$, and Ejection Fraction f of the Mixing Region), the Outputs (Remnant Mass $M_{\rm rem}$ and Ejected Iron Mass $M(^{56}{\rm Ni})$), and the χ^2 of the Abundance Fitting

Name	[Fe/H] (dex)	[Mg/Fe] (dex)	[Ca/Fe] (dex)	M ($M_\odot$)	E_{51} (10^{51} erg)	$M_{\rm cut}$ ($M_\odot$)	$M_{\rm mix}$ ($M_\odot$)	log f	$M_{\rm rem}$ ($M_\odot$)	$M(^{56}{\rm Ni})$ ($M_\odot$)	χ^2/N
J144256−001542	-4.09 ± 0.21	0.27	0.29	15	1	1.5	···	0.0	1.5	0.06	0.12
				15	1	1.4	1.5	−1.2	1.5	0.06	0.12
				25	1	1.7	2.9	−0.4	2.4	0.10	<0.01
				40	30	2.2	5.9	−0.8	5.3	0.33	<0.01
J153346+155701	-3.34 ± 0.26	0.06	0.08	15	1	1.4	···	0.0	1.4	0.14	0.38
				15	1	1.4	1.5	−0.3	1.4	0.09	0.09
				25	1	1.7	3.6	−0.3	2.6	0.13	0.19
				25	10	1.8	3.5	−0.4	2.8	0.24	<0.01
J161956+170539	-3.57 ± 0.25	0.04	−0.35	15	1	1.4	3.2	−4.0	3.2	1.4×10^{-5}	0.30
				25	10	1.7	6.5	−4.0	6.5	6.7×10^{-5}	0.71
HE0305−5442	-3.30 ± 0.20	0.22	−0.04	15	1	1.4	1.6	−0.5	1.5	0.04	1.37
				25	10	1.7	6.2	−1.6	6.1	0.02	1.14
HE1416−1032	-3.20 ± 0.16	0.18	0.03	15	1	1.4	4.3	−2.4	4.3	5.4×10^{-4}	3.10
				25	10	1.9	9.1	−3.6	9.1	1.3×10^{-4}	3.67
HE2356−0410	-3.06 ± 0.20	0.11	0.16	15	1	1.4	3.1	−3.7	3.1	2.7×10^{-5}	8.64
				25	10	1.9	7.1	−4.7	7.1	1.0×10^{-5}	6.01

larger $M_{\rm mix}$ and/or larger f values could also give lower [α/Fe] ratios. To be consistent with observed supernovae, 40 $M_\odot$ supernova models require unrealistically extended mixing and large fallback ($M_{\rm mix} > 8\,M_\odot$ and $f < 0.2$). Among hypernovae, 25 $M_\odot$ models give a slightly better fit than 40 $M_\odot$ models.

SDSS J161956+170539—This star shows a carbon enhancement, and thus the enrichment source should be faint supernovae (dotted line) or faint hypernovae (dashed line). A large fraction of material in the mixing region falls back onto a remnant, and thus the ejected iron mass is smaller than $M({\rm Fe}) = 0.001\,M_\odot$. If there is no such large fallback, the [C/Fe] ratio becomes too small (solid line). This is the case for models of other CEMP stars at [Fe/H]$\lesssim -3$, independent of the [α/Fe] ratios. In order to reproduce the observed low [Mg/Fe] ratio, it is necessary that the progenitor mass is lower than that for other CEMP stars, or that there is more extended mixing and larger fallback ($M_{\rm mix} \gtrsim 8\,M_\odot$). Among α elements, [(Si, Ca)/(O, Mg)] ratios tend to be higher for massive stars. Therefore, 25–40 $M_\odot$ supernova/hypernova models may produce [Si/Fe] and [Ca/Fe] ratios larger than the observed ratios. In any case, the remnant mass is as massive as $M_{\rm rem} \sim 5\,M_\odot$, which is in the range of black holes. Although the M(Fe) in Table 1 may be too small to make a star with [Fe/H] ~ -3, there are acceptable models that have $M({\rm Fe}) \sim 10^{-4}\,M_\odot$ with $\chi^2/N = 0.30$ and 0.86 for 15 and 25 $M_\odot$ models, respectively.

To put a further constraint on the models of enrichment sources with abundance fitting, it is necessary to use the elemental abundances of iron-peak elements. We also apply the abundance fitting to a subset of the sample from Cohen et al. (2013) that have [Fe/H] < -3, low [Mg/Fe] < 0.25, and high signal-to-noise ratios, S/N > 80. This set includes four stars (HE2357−0701, HE1416−1032, HE0305−5442, and BS16467−062 with [Mg/Fe] = 0.12, 0.18, 0.22, and 0.24, respectively) that do not show carbon enhancement, and one CEMP-low-α star (HE2356−0410 with [Mg/Fe] = 0.11) that is similar to Caffau et al.'s (2013) CEMP star. Figure 2 shows the comparison of the elemental abundance patterns between observations and favored models. NLTE corrections are included for Al observations (+0.6, Cohen et al. 2013), but not for Na (~ -0.2 to -0.5), and we apply a constant shift of +0.2 for Cr I (Lai et al. 2008), but not for Mn I ($\sim +0.3$).

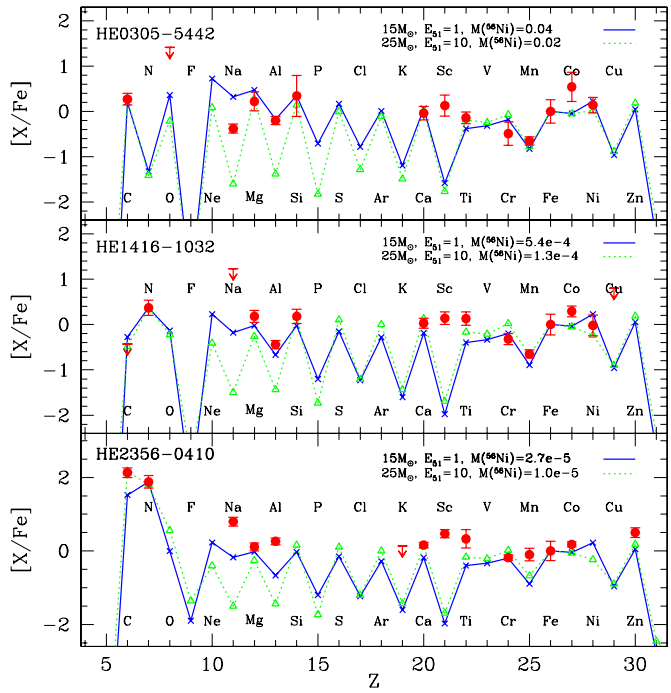

Figure 2. Elemental abundance patterns of three EMP stars with (top and middle panels) and without (bottom panel) carbon enhancement from Cohen et al. (2013). In the top and middle panels, the solid and dotted lines show the nucleosynthesis yields of a low-mass supernova and hypernova, respectively. In the lower panel, the solid and dotted lines are for a faint supernova and faint hypernova, respectively. All models are with mixing-fallback.

(A color version of this figure is available in the online journal.)

For all of the five low [Mg/Fe] stars, the abundance patterns can be reproduced with core-collapse supernovae, i.e., (1) 13–15 $M_\odot$ supernovae, (2) 13–40 $M_\odot$ supernovae with mixing-fallback, or (3) hypernovae, except for the following elements. Sc, Ti, V, and Co yields depend on the density structure of progenitor stars (Tominaga et al. 2007b), and can be larger with two-dimensional explosions (Tominaga 2009). Mn and Co yields depend on $Y_{\rm e}$ that can vary due to the neutrino process during the explosion. Co and Zn yields depend on

the explosion energy (Umeda & Nomoto 2005; Kobayashi et al. 2006; Tominaga et al. 2007b). N, Na, and Al yields depend not only on the existence of rotation, but also on the degree of mixing of hydrogen during hydrostatic burning. In our abundance fitting, Na, Al, K, Sc, and Ti are excluded.

For all five stars, compared with other models, 40 $M_\odot$ supernova models show stronger odd-Z effects. In particular, [Co/Fe] ratios are much lower than in 13–25 $M_\odot$ supernova models and hypernova models. This relative difference in [Co/Fe] among models will remain, although the absolute amounts of Co yields should be increased with multi-dimensional explosions with the neutrino process. Therefore, 40 $M_\odot$ supernova models are strongly disfavored from the observed Co abundances. Among the four non-CEMP stars, HE1416−1032 and HE2357−0701 show some nitrogen enhancement with ([N/Fe], [N/C]) = (0.37, >0.80) and (0.87, 0.61), respectively. This nitrogen enhancement could be explained with faint supernova/hypernova models. We should note, however, that the C and N abundances may be affected by internal mixing (e.g., Spite et al. 2005). For the CEMP star, the enrichment source should be faint supernovae/hypernovae. In most of the cases, C/O is lower, Si/O is higher, (Cr, Mn)/Fe are lower, and (Co, Zn)/Fe are higher for 40 $M_\odot$ hypernova models than for 13–15 $M_\odot$ supernova models. This observed high [Zn/Fe] ratio can be realized only with hypernova models, i.e., with even higher explosion energies. Note that the observed [Mn/Fe] ratio may be higher than in our models, which could be explained with the variation of Y_e due to the neutrino process.

There are other low-α EMP stars in the literature. In Yong et al. (2013), 13 out of 47 stars show [Mg/Fe] < 0.2, although Zn abundances are not available. In Barklem et al. (2005), 57 out of 253 stars show [Mg/Fe] < 0.2, although the data quality is not as good as in Cohen et al. (2013) and Yong et al. (2013). Among the 57 stars, 7 stars show high [Zn/Fe] > 0.3, including HE0547−4539 at [Fe/H] = −3.01, indicating hypernovae, while 6 stars do not show such Zn enhancement, and may be consistent with 13–25 $M_\odot$ supernovae.

3. DISCUSSION

The variation of the [α/Fe] ratios of EMP stars is known. Kobayashi et al. (2000) commented that some anomalous stars that have low [α/Fe] at [Fe/H] $\lesssim -1$ can be explained not by SNe Ia but by 13–15 $M_\odot$ core-collapse supernovae. Argast et al. (2002) showed that the predicted [α/Fe] ratios have a too large scatter in stochastic models of chemical evolution with the yields from Nomoto et al. (1997). In the updated yields of Kobayashi et al. (2006), the ejected iron mass M(Fe) was constrained from the observations of supernovae (Nomoto et al. 2003). As a result, M(Fe) was decreased in low-mass supernovae and increased in high-mass supernovae. Therefore, the intrinsic variation of [α/Fe] became much smaller in Kobayashi et al. (2006) than in Nomoto et al. (1997). In chemodynamical simulations with the updated yields, the scatter of [α/Fe] is comparable to observations (Figure 13 of Kobayashi & Nakasato 2011).

The mixing-fallback effect is naturally expected in the case of hypernovae, which are jet-induced explosions followed by black hole formation (Tominaga et al. 2007a; Tominaga 2009). In hypernovae, large fallback is possible even for such energetic explosions as $E_{51} \gtrsim 10$ if the timescale of jet injection is long (Tominaga et al. 2007a). In supernovae, it is also possible that some degree of mixing occurs through Rayleigh–Taylor instability (e.g., Hachisu et al. 1990; Joggerst et al. 2009). Hachisu et al. (1991) showed that more massive supernovae tend to undergo less extended Rayleigh–Taylor mixing (i.e., smaller $M_{\rm mix}$) because of the smaller deceleration of the expanding core due to smoother density structures.

The origin of CEMP-low-α stars is interesting. If there is a CEMP-low-α star with [Zn/Fe] ∼ [Co/Fe] ∼ 0, that would require a new population, i.e., ∼10–20 $M_\odot$ faint supernovae that form black holes. For $\lesssim$20 $M_\odot$ stars, they are believed to form neutron stars, and thus black-hole forming faint supernovae have not been discussed in previous works.

On the other hand, ∼10–20 $M_\odot$ supernovae are not rare. Because they have an ejection mass smaller than that of more massive stars, the contribution from ∼10–20 $M_\odot$ supernovae can appear at various metallicities in the system where chemical enrichment took place inhomogeneously. One example may be dwarf spheroidal galaxies (dSphs). It is known that stars in dSphs have lower [α/Fe] than stars in the solar neighborhood at a given metallicity (e.g., Tolstoy et al. 2009), and some EMP stars in dSphs also show low [α/Fe] (Aoki et al. 2009). This is sometimes explained by contribution from SNe Ia with a longer timescale of star formation (if the SN Ia lifetimes do not depend on the progenitor metallicity). However, the elemental abundance patterns, in particular the [Mn/Fe] ratios as low as those of halo stars (North et al. 2012), are not consistent with the enrichment from SNe Ia. In small systems such as dSphs, it is likely that the star formation efficiency is low and thus the sampling of massive stars is incomplete, which results in the missing contribution from massive stars at $\gtrsim$20 $M_\odot$ (Kobayashi et al. 2006; Nomoto et al. 2013; see also McWilliam et al. 2013). In the Milky Way galaxy, similar abundance patterns was reported by Nissen & Schuster (2010, 2011), which tend to be accreted halo stars from their kinematics. Ishigaki et al. (2012) also showed that stars with Galactic outer halo kinematics tend to have low [α/Fe] ratios. For such an accretion component, incomplete sampling of massive stars is possible, although the metallicity is higher than that of EMP stars. The abundance patterns of these stars are also consistent with our 13–25 $M_\odot$ supernova models.

Abundance fitting is a new approach to study the properties of supernovae. Statistical studies with a large homogeneous sample will be able to answer the following questions: what is the major source of chemical enrichment in the early universe? Namely, what are the distribution functions of progenitor mass, ejected iron mass, and explosion energy of supernovae? Are the mass–energy and mass–iron mass relations of nearby supernovae reproduced? What is the mass function of the remnants of the first stars?

4. CONCLUSIONS

In the early stages of chemical enrichment, the interstellar medium is supposed to be highly inhomogeneous, so that the properties of the first supernovae can be directly extracted from the comparison between the observed elemental abundances and nucleosynthesis yields. We show that the low [α/Fe] ratios recently found for a small fraction of extremely metal-poor stars can be naturally explained with the nucleosynthesis yields of core-collapse supernovae, i.e., (1) 13–25 $M_\odot$ supernovae or (2) hypernovae. If we allow an enhanced mixing and a large fallback, 40 $M_\odot$ supernova models (3) could be consistent with the observed low [α/Fe] ratios. For the case without carbon enhancement, the ejected iron masses of these favored models (1–3) are normal, M(Fe) = 0.05–0.15 $M_\odot$ for supernovae and M(Fe) = 0.1–1.4 $M_\odot$ for hypernovae, consistent with observed light curves and spectra of nearby supernovae. The first source

(1) has been included in the standard set of nucleosynthesis yields that have been applied to galactic chemical evolution models, while the other sources are different from those in galactic chemical evolution models and are rarer.

On the other hand, the carbon enhancement requires much smaller iron production, and the low $[\alpha/\mathrm{Fe}]$ of carbon-enhanced metal-poor stars can also be reproduced with faint supernovae or faint hypernovae. The ejected iron mass is $M(\mathrm{Fe}) < 0.001\ M_\odot$, much smaller than normal supernovae. These enrichment sources are similar to those proposed for typical carbon-enhanced EMP stars and DLAs with $[\alpha/\mathrm{Fe}] \gtrsim 0.5$, but the progenitor mass is as low as 13–25 $M_\odot$, or more extended mixing and larger fallback occur in 25–40 $M_\odot$ stars. The former case implies that $\lesssim$25 $M_\odot$ stars may form black holes.

Iron-peak element abundances, in particular Zn abundances, are important to put further constraints on the enrichment sources. 25–40 $M_\odot$ supernova (not hypernova) models may disagree with the observed high Co abundances of low $[\alpha/\mathrm{Fe}]$ stars. The frequency of these sources should be examined with future galactic archaeology surveys.

We would like to thank E. Caffau and P. Bonifacio for providing their results prior to publication. We are grateful to A. Bunker for fruitful discussion. This work has been supported in part by the WPI Initiative, MEXT, Japan, and by the Grant-in-Aid for Scientific Research of the JSPS (18104003, 20540226) and MEXT (19047004, 22012003).

REFERENCES

Andrievsky, S. M., Spite, M., Korotin, S. A., et al. 2010, A&A, 509, 88
Aoki, W. 2010, in IAU Symp. 265, Chemical Abundances in the Universe: Connecting First Stars to Planets, ed. K. Cunha et al. (Cambridge: Cambridge Univ. Press), 111
Aoki, W., Arimoto, N., Sadakane, K., et al. 2009, A&A, 502, 569
Argast, D., Samland, M., Thielemann, F.-K., & Gerhard, O. E. 2002, A&A, 388, 842
Audouze, J., & Silk, J. 1995, ApJL, 451, L49
Barklem, P. S., Christlieb, N., Beers, T. C., et al. 2005, A&A, 439, 129
Beers, T. C., & Christlieb, N. 2005, ARA&A, 43, 531
Caffau, E., Bonifacio, P., François, P., et al. 2011, Natur, 477, 67
Caffau, E., Bonifacio, P., François, P., et al. 2013, A&A, 560, 15
Cayrel, R., Depagne, E., Spite, M., et al. 2004, A&A, 416, 1117
Cohen, J. G., Christlieb, N., Thompson, I., et al. 2013, ApJ, 778, 56
Hachisu, I., Matsuda, T., Nomoto, K., & Shigeyama, T. 1990, ApJL, 358, L57
Hachisu, I., Matsuda, T., Nomoto, K., & Shigeyama, T. 1991, ApJL, 368, L27
Honda, S., Aoki, W., Kajino, T., et al. 2004, ApJ, 607, 474
Ishigaki, M. N., Chiba, M., & Aoki, W. 2012, ApJ, 753, 64
Iwamoto, N, Umeda, H., Tominaga, N., Nomoto, K., & Maeda, K. 2005, Sci, 309, 451
Joggerst, C. C., Woosley, S. E., & Heger, A. 2009, ApJ, 693, 1780
Kobayashi, C., Karakas, I. A., & Umeda, H. 2011, MNRAS, 414, 3231
Kobayashi, C., & Nakasato, N. 2011, ApJ, 729, 16
Kobayashi, C., & Nomoto, K. 2009, ApJ, 707, 1466
Kobayashi, C., Tominaga, N., & Nomoto, K. 2011, ApJL, 730, L14
Kobayashi, C., Tsujimoto, T., & Nomoto, K. 2000, ApJ, 539, 26
Kobayashi, C., Umeda, H., Nomoto, K., Tominaga, N., & Ohkubo, T. 2006, ApJ, 653, 1145
Kroupa, P. 2008, in ASP Conf. Ser. 390, Pathways through an Eclectic Universe, ed. J. H. Knapen, T. J. Mahoney, & A. Vazdekis (San Francisco, CA: ASP), 3
Lai, D. K., Bolte, M., Johnson, J. A., et al. 2008, ApJ, 681, 1524
Lugaro, M., de Mink, S. E., Izzard, R. G., et al. 2008, A&A, 484, 27
McWilliam, A., Wallerstein, G., & Mottini, M. 2013, ApJ, 778, 149
Meynet, G., Ekström, S., & Maeder, A. 2006, A&A, 447, 623
Nissen, P. E., & Schuster, W. J. 2010, A&A, 511, 10
Nissen, P. E., & Schuster, W. J. 2011, A&A, 530, 15
Nomoto, K., Hashimoto, M., Tsujimoto, T., et al. 1997, NuPhA, 616, 79c
Nomoto, K., Kobayashi, C., & Tominaga, N. 2013, ARA&A, 51, 457
Nomoto, K., Maeda, K., Umeda, H., et al. 2003, in IAU Symp. 212, A Massive Star Odyssey, from Main Sequence to Supernova, ed. V. D. Hucht et al. (San Francisco, CA: ASP), 395
North, P., Cescutti, G., Jablonka, P., et al. 2012, A&A, 541, 45
Smartt, S. J. 2009, ARA&A, 47, 63
Spite, M., Cayrel, R., Plez, B., et al. 2005, A&A, 430, 655
Suda, T., Aikawa, M., Machida, M. N., et al. 2004, ApJ, 611, 476
Tolstoy, E., Hill, V., & Tosi, M. 2009, ARA&A, 47, 371
Tominaga, N. 2009, ApJ, 690, 526
Tominaga, N., Maeda, K., Umeda, H., et al. 2007a, ApJL, 657, L77
Tominaga, N., Umeda, H., & Nomoto, K. 2007b, ApJ, 660, 516
Umeda, H., & Nomoto, K. 2002, ApJ, 565, 385
Umeda, H., & Nomoto, K. 2005, ApJ, 619, 427
Yong, D., Norris, J. E., Bessell, M. S., et al. 2013, ApJ, 762, 27